• Basic Research •

Trimethylamine N-oxide aggravates vascular permeability and endothelial cell dysfunction under diabetic condition: *in vitro* and *in vivo* study

Jia-Yi Jiang[1], *Wei-Ming Liu*[1], *Qiu-Ping Zhang*[2], *Hang Ren*[1], *Qing-Ying Yao*[1], *Gao-Qin Liu*[1], *Pei-Rong Lu*[1]

[1]Department of Ophthalmology, the First Affiliated Hospital of Soochow University, Suzhou 215006, Jiangsu Province, China
[2]Suzhou Center for Disease Prevention and Control, Suzhou 215004, Jiangsu Province, China
Co-first authors: Jia-Yi Jiang and Wei-Ming Liu
Correspondence to: Pei-Rong Lu. Department of Ophthalmology, the First Affiliated Hospital of Soochow University, 188 Shizi Street, Suzhou 215006, Jiangsu Province, China. lupeirong@suda.edu.cn
Received: 2023-03-26 Accepted: 2023-10-30

Abstract

● **AIM:** To provide the direct evidence for the crucial role of trimethylamine N-oxide (TMAO) in vascular permeability and endothelial cell dysfunction under diabetic condition.

● **METHODS:** The role of TMAO on the *in vitro* biological effect of human retinal microvascular endothelial cells (HRMEC) under high glucose conditions was tested by a cell counting kit, wound healing, a transwell and a tube formation assay. The inflammation-related gene expression affected by TMAO was tested by real-time polymerase chain reaction (RT-PCR). The expression of the cell junction was measured by Western blotting (WB) and immunofluorescence staining. In addition, two groups of rat models, diabetic and non-diabetic, were fed with normal or 0.1% TMAO for 16wk, and their plasma levels of TMAO, vascular endothelial growth factor (VEGF), interleukin (IL)-6 and tumor necrosis factor (TNF)-α were tested. The vascular permeability of rat retinas was measured using FITC-Dextran, and the expression of zonula occludens (ZO)-1 and claudin-5 in rat retinas was detected by WB or immunofluorescence staining.

● **RESULTS:** TMAO administration significantly increased the cell proliferation, migration, and tube formation of primary HRMEC either in normal or high-glucose conditions. RT-PCR showed elevated inflammation-related gene expression of HRMEC under TMAO stimulation, while WB or immunofluorescence staining indicated decreased cell junction ZO-1 and occludin expression after high-glucose and TMAO treatment. Diabetic rats showed higher plasma levels of TMAO as well as retinal vascular leakage, which were even higher in TMAO-feeding diabetic rats. Furthermore, TMAO administration increased the rat plasma levels of VEGF, IL-6 and TNF-α while decreasing the retinal expression levels of ZO-1 and claudin-5.

● **CONCLUSION:** TMAO enhances the proliferation, migration, and tube formation of HRMEC, as well as destroys their vascular integrity and tight connection. It also regulates the expression of VEGF, IL-6, and TNF-α.

● **KEYWORDS:** diabetic model; trimethylamine N-oxide; inflammation; endothelial dysfunction; rats; retinal microvascular endothelial cells

DOI:10.18240/ijo.2024.01.04

Citation: Jiang JY, Liu WM, Zhang QP, Ren H, Yao QY, Liu GQ, Lu PR. Trimethylamine N-oxide aggravates vascular permeability and endothelial cell dysfunction under diabetic condition: *in vitro* and *in vivo* study. *Int J Ophthalmol* 2024;17(1):25-33

INTRODUCTION

Diabetic retinopathy (DR) is one of the most common complications of diabetes, and its prevalence has become a heavy medical and social burden worldwide[1]. The development and progression of DR is mainly related to the duration of diabetes, blood glucose level[2], blood pressure[3], blood lipid level[4], *etc*. The early stage of DR features neurodegeneration and vascular lesions, including endothelial cells and pericyte loss, a damaged blood-retina barrier (BRB) and the formation of microaneurysms. The management of DR has been a focal point of interest in research. Nevertheless, there are few effective options to prevent or slow development in the early stage. Therefore, there is still an urgent need for a better understanding of the pathogenesis and the related risk factors of DR.

Trimethylamine N-oxide (TMAO) is a tertiary aliphatic amine derived from choline and carnitine intake. After gut microbiota

metabolism, trimethylamine (TMA) is absorbed through the gut barrier and transferred to TMAO in the liver *via* flavin monooxygenases (FMO). TMAO is mainly excreted in urine, with a small amount excreted in sweat and breath[5]. Western diets rich in red meat and fat are related to higher plasma TMAO levels[6]. Some studies have suggested that TMAO is responsible for a higher risk of atherosclerosis[7], in which endothelial dysfunction plays a vital role. TMAO exposure leads to monocyte adhesion and endothelial cell aberrance[8], and it also promotes vascular inflammation by activating the nucleotide-binding oligomerization domain-like receptor 3 (NLRP3) inflammasome[9]. However, the influence of TMAO on the microvascular system remains unclear. A substantial number of studies have revealed a positive dose-dependent association between circulating TMAO levels and increased risk of obesity and diabetes[10]. Our previous research has demonstrated that elevated plasma TMAO concentration is associated with a larger chance of DR[11]. We propose that TMAO plays a deleterious role in DR by inducing endothelial cell dysfunction and microvascular system abnormalities.

In this study, we reveal that TMAO promotes abnormal variations of human retinal microvascular endothelial cells (HRMEC) and that it also aggravates hyperglycaemia-related impairment in the retinal vascular system of diabetic rats.

MATERIALS AND METHODS

Ethical Approval All animal experiments were approved by the Animal Care Committee of Soochow University and conformed to the protocol of the Care and Use of Experimental Animals. We conducted all animal experiments adhering to the ARVO Statement for the use of Animals in Ophthalmic and Vision Research. All experiments with animals complied with the institutional protocols on animal welfare and were approved by the Ethics Committee of Soochow University and the approval number was SUDA20221223A16.

Cell Culture and Treatment HRMEC (cat no. ABC-TC3789, Qida, Shanghai, China) were cultured in an endothelial cell medium (1001, Sciencell, Carlsbad, CA, USA) containing 5% foetal bovine serum, 1% endothelial cell growth supplement and 100 U/mL penicillin/streptomycin at 37℃ and 5% CO_2. HRMEC were treated with medium with 25 mmol/L glucose (high glucose, HG) or treated with 5.5 mmol/L glucose (normal glucose, NG) for the indicated time.

HRMEC Proliferation Assay The proliferation of HRMEC was measured by cell counting kit-8 (CCK8) assay. HRMEC were seeded into 96-well plates at 5000 cells per well. When the cells reached 70% confluence, the medium was replaced by serum-free medium of NG or HG, supplemented with or without 100, 500, or 1000 μmol/L TMAO, and an additional group of isotonic controls (NG with 20 mmol/L mannitol), in triplicate. After 24h of culture, a 10 mL CCK8 solution was added to each well and incubated for 2h before the absorbance was evaluated at a 450 nm wavelength.

HRMEC Wound Healing Assay, Transwell Assay and Tube Formation Assay To evaluate the migration ability of HRMEC, the wound healing assay and transwell assay were conducted. The cells were seeded into 6-well plates and grown to confluence. A peptide tip was used to create a scratch before the indicated treatment 24h and 48h before images were taken. The lengths of scratches were assessed by Image J software (NIH, USA). Each well was randomly scribed with 6-8 lines perpendicular to the scratch, and the average value of the measurement was regarded as the scratch distance. The difference in width compared to 0h represents the cell migration distance.

A transwell assay was conducted to determine cell longitudinal migration. The transwell chambers were placed into 24-well plates, and the lower wells were supplemented with a normal glucose medium with (0 or 500 μmol/L) TMAO and a high-glucose medium with (0 or 500 μmol/L) TMAO. HRMEC suspension at a density of 7.5×10^4 cells/well were seeded in the upper chamber. After 24h incubation, the cells in the upper chamber were swept and the cells in the lower chambers were stained with gentian violet. Three to five fields were randomly obtained from each cell for quantification.

Tube formation assays were used to assess the vessel generation ability of HRMEC. Matrigel was thawed at 4℃ overnight and added to 96-well plates on ice to avoid bubble formation. After centrifuging at 1200 rpm for 5min, the plates were incubated at 37℃ for 1h of preparation. HRMEC were seeded in wells and incubated for 6h before images were taken. The capillary was quantified by measuring the total number of tube structures under a 40× bright-field microscope.

Real-Time Polymerase Chain Reaction Total RNA was extracted with TRIzol reagent (15596018, Invitrogen) and cDNA was synthesized using the PrimeScrip RT reagent Kit (RR037A, Takara) according to the manufacturer's instructions. RT-PCR was performed in triplicate using a Roche LightCycler 480 Instrument II with TB Green™ Premix Ex Taq™ (RR420A, Takara, Japan). The expression of the gene of interest was normalized to the housekeeping gene GAPDH using the $2^{-\Delta\Delta Ct}$ method. All the RT-PCR primers used are listed in Table 1.

Immunofluorescence Staining Cultured HRMEC were fixed with 4% paraformaldehyde for 10min at room temperature, permeabilized for 30min with 0.25% Triton X-100 and blocked for 40min. Cells were incubated with the primary antibody zonula occludens (ZO)-1 (21773-1-AP, Proteintech) overnight at 4℃ and followed by the secondary antibody goat anti-rabbit

Table 1 List of primers used in RT-PCR

Primers	Sequence, 5'-3'
ICAM-1	F: CCAGGAGACACTGCAGACAG R: CTTCACTGTCACCTCGGTCC
MCP-1	F: CAGCCAGATGCAATCAATGCC R: TGGAATCCTGAACCCACTTCT
IL-1β	F: AGCTACGAATCTCCGACCAC R: CGTTATCCCATGTGTCGAAGAA
TNF-α	F: AAGGACACCATGAGCACTGAA R: GGAGAAGAGGCTGAGGAACAA
MMP-2	F: TACAGGATCATTGGCTACACACC R: GGTCACATCGCTCCAGACT
NLRP3	F: AAGGCCGACACCTTGATATG R: CCGAATGTTACAGCCAGGAT
VEGF-A	F: CTTGCCTTGCTGCTCTACC R: ACACAGGATGGCTTGAAGATG
β-actin	F: GCCGTCTTCCCCTCCATCGTG R: TCTCTTGCTCTGGGCCTCGTC

ICAM-1: Intercellular adhesion molecule 1; MCP-1: Monocyte chemoattractant protein 1; IL-1β: Interleukin 1 beta; TNF-α: Tumor necrosis factor alpha; MMP-2: Matrix metallopeptidase 2; NLRP3: Nucleotide-binding oligomerization domain-like receptors 3; VEGF-A: Vascular endothelial growth factor A.

Alexa Fluor® 488-IgG (ab150077, Abcam) at a 1:500 dilution for 2h at room temperature. The nuclei were stained with DAPI (D9542, Sigma-Aldrich) at room temperature for 15min. The images were obtained with an FV3000 confocal microscope (Olympus, Japan).

Animals' Treatment Male Sprague Dawley (SD) rats (6wk; 180-200 g) were purchased from Shanghai SLAC Laboratory Animal Co., Ltd., China. The rats were housed at 22℃-26℃ and 50%-60% humidity, and they had free access to chow and water. The rats were randomly divided into two groups: one was intraperitoneally injected with 60 mg/kg of streptozocin (STZ, Sigma-Aldrich) dissolved in saline sodium citrate after overnight fasting, and the other was injected with equal quantity of citrate buffer. A week later, the blood from the rats' tail veins was monitored, and rats with blood glucose higher than 16.7 mmol/L were considered as successful diabetic models and recruited into the diabetic group (D group) or the diabetic with TMAO treatment group (D+T group). After grouping, the D and D+T groups showed similar blood sugar levels, and the differences between them were less than 1.1 mmol/L. Rats that accepted the citrate buffer were randomly set to a negative control (NC group) or TMAO-feeding group (T group). The NC and D groups had access to standard drinking water, while the T and D+T groups received drinking water containing 0.1% TMAO[12-14]. The rats were sacrificed 16wk later.

Quantification of Plasma TMAO and Cytokine Concentrations The rat blood samples were collected into EDTA-treated tubes and immediately centrifuged at 4℃ and 4000 g for 10min before being stored at -80℃. At the time of analysis, samples were thawed at 4℃ and measured by liquid chromatography-tandem mass spectrometry (LC-MS/MS) as described[11]. Each sample with 50 mL was mixed with 200 mL of methanol containing 500 mg/L internal standard d_9-TMAO, vortex for 30s and centrifuged at 4℃, 12 000 rpm for 10min for the supernatant. After a repeat centrifugation, the supernatant was moved into a sampling bottle and analysed. The levels of interleukin (IL)-6, tumor necrosis factor (TNF)-α and vascular endothelial growth factor (VEGF) were measured with their respective kits (MLBio, Shanghai, China) according to the manufacturer's instructions.

***In Vivo* Permeability Assay** To assess the inner blood-retinal barrier (iBRB) integrity, the permeability assay was used following procedure previously reported with minor modifications[15-16]. After anaesthesia, FITC-Dextran solution was injected into the left ventricle of rats from each group at 30 mg/kg body weight. Five minutes later, the eyes were enucleated and fixed in 4% formalin on ice for 2h. After fixation, the retinas were carefully stripped and moved to slides for photography. Representative images were captured with 10× objective of FV3000 confocal microscope (Olympus, Japan). Ten representative images from each rat were captured using a 20× objective of confocal microscopy, and leakage areas showing as diffused fluorochrome from retinal capillaries were analysed automatically by Image J (National Institutes of Health).

Western Blot The lysates from HRMEC and the retinal tissues were prepared using cell lysis (9803S, Cell Signalling Technology) for Western blotting (WB). The concentration of protein samples was examined using a BCA protein assay kit (23225, Thermo Scientific). The antibodies used include ZO-1 (21773-1-AP, Proteintech), occludin (27260-1-AP), claudin-5 (AF5216, Affinity), VEGF (19003-1-AP, Proteintech), GAPDH (60004-1, Proteintech), and secondary antibodies (7074S, 7076S, Cell Signalling Technology).

Statistical Analysis Each assay was performed at least three times. The results of three replicate experiments in ELISA are summed up and presented in a single graph for statistical analysis. The remaining figures show representative results from the three replicates. The representative data are presented as mean±standard error of mean (SEM). Student's *t*-test and one-way ANOVA using GraphPad Prism 9 Software were used for statistical analysis. The general acceptance of significance was $P<0.05$.

RESULTS

TMAO Coordinated with High Glucose to Promote HRMEC Proliferation, Migration, and Tube Formation Proliferation, migration, and tube formation are hallmarks of the angiogenesis function of vascular endothelial cells. To examine the effect of TMAO on retina vessels individually and under hyperglycaemic conditions, we treated HRMEC in NG

(5.5 mmol/L) with 0, 100, 500, and 1000 μmol/L TMAO, and HG (25 mmol/L) with 0, 100, 500, and 1000 μmol/L TMAO for 24h. To exclude the interference of osmotic factor, 5.5 mmol/L glucose media with 20 mmol/L mannitol was used as a control. Compared with normal glucose, 500 and 1000 μmol/L TMAO significantly increased the HRMEC proliferation rate (P<0.05). HG also promoted HRMEC proliferation, and 500 and 1000 μmol/L TMAO further increased HRMEC proliferation (P<0.05; Figure 1A).

The migration ability of HRMEC under NG and HG with TMAO was determined by a wound healing assay and a transwell assay. Totally 500 μmol/L TMAO and HG both significantly augmented migration of HRMEC, but the effect was more significant under HG with 500 μmol/L TMAO (P<0.05; Figure 1B-1C). Transwell assay revealed that the migration ability of HRMEC was enhanced in NG+TMAO, HG and HG+TMAO compared with NG group, among which HG+TMAO identified the highest migration rate (P<0.05; Figure 1D-1E).

To examine the vascular formation ability of HRMEC, after 6h treatment, the capillary-like structure was calculated under NG, NG+TMAO, HG and HG+TMAO and the number of tube structures was increasingly elevated (P<0.05; Figure 1F-1G). Therefore, it can be inferred that TMAO promoted HRMEC proliferation, migration, invasion, and tube formation, coordinating with the effect of high glucose.

TMAO Aggravated High Glucose-Induced Inflammation and Cell Junction Loss in HRMEC An RT-PCR analysis revealed that TMAO and HG treatment both significantly increased the mRNA expression levels of inflammation, adhesion, and angiogenesis genes, including IL-1β, TNF-α, NLRP3, monocyte chemoattractant protein 1 (MCP-1), intercellular adhesion molecule 1 (ICAM-1), matrix metallopeptidase 2 (MMP-2), and VEGF-A in HRMEC compared to the NG group (P<0.05). HG with TMAO supplementation further increased the expression of the above-mentioned genes (P<0.05; Figure 2A).

The iBRB is composed of retinal capillary endothelial cells, and its integrity ensures the separate flow of retina and blood constituents and exchange of substances. To identify the role of TMAO in iBRB function, the expression levels of tight junction proteins ZO-1 and occludin in HRMEC were analysed by WB and immunofluorescence staining. Compared with NG, ZO-1 and occludin expression gradually decreased after treatment with NG+500 μmol/L TMAO, HG, and HG+500 μmol/L TMAO (Figure 2B-2C; P<0.05). Similarly, the immunofluorescence staining also indicated that HG inhibited ZO-1 expression, and TMAO exaggerated its effect (Figure 2D).

Circulating TMAO Elevated in Diabetic Rats and Induced Systemic Inflammation To better understand the action of TMAO in DR, an STZ-induced diabetic rat model was used. All groups were fed standard chow, the D and D+T groups were induced to be diabetic and the T and D+T groups were supplied with 0.1% TMAO in drinking water. The body weight of the NC and TMAO groups gradually increased to 597±30 and 594±20 g, while the D and D+T groups remained at a steadily low level of 181±19 and 193±20 g, respectively. Both showed significant decreases compared with the NC group (P<0.001; Figure 3A). Meanwhile, the blood glucose of the NC and T groups were stable at 7±1 mmol/L, but the D and D+T groups saw a gradual elevation from the onset of hyperglycaemia at 21±3 and 20±2 mmol/L to 28±4 and 29±3 mmol/L, respectively, after 16wk; both increased significantly compared with the NC group (P<0.001; Figure 3B).

When the rats were sacrificed at 16wk, plasma was obtained for TMAO evaluation. The circulating TMAO level was 0.78±0.13 μmol/L in the NC group, which was significantly lower than 1.68±0.62 μmol/L in the T group (P<0.001). Meanwhile, the D group and D+T group showed sharp increase compared with the NC group (P<0.0001), at 6.82±2.39 and 25.20±5.50 μmol/L, respectively (Figure 3C). These data revealed that diabetes was related to higher levels of TMAO, and TMAO intake caused higher circulating TMAO, especially under diabetic conditions. However, TMAO intake had no influence on body weight and blood glucose level, as they showed similar trends in the D and D+T groups (P>0.05), suggesting that TMAO may act as an individual risk factor beyond glucose.

Circulating inflammatory cytokines have a considerable influence on retinal vascular permeability. We examined plasma cytokine levels, including VEGF, TNF-α, and IL-6. Notably, dietary TMAO intake augmented TNF-α, IL-6 and VEGF levels in plasma (P<0.01 for all). In the diabetic group, TNF-α (P<0.05), IL-6 (P<0.01) and VEGF (P<0.01) were significantly increased. Increasing trends were also identified in the TMAO supplement, although no significance was found (Figure 3D-3F). These results implied that an increase in TMAO led to an alteration in the inflammation network and VEGF, thus enhancing vascular permeability.

TMAO Aggravated Diabetic Retinopathy by Inducing Vascular Leakage and Destructing Cell Junction Proteins *In Vivo* The early stage of diabetic retina damage features tight junction impairment and vascular leakage. Therefore, we then evaluated retinal vessel integrity through FITC-Dextran perfusion. Retinal vasculature of diabetic rats showed a significant increase in leakage area compared with the NC group (P<0.05). Moreover, in the TMAO supplement, the leakage area of the D+T group was even higher compared with to NC group (P<0.01); it showed an increasing trend compared to the D group (Figure 4). The results from WB analysis

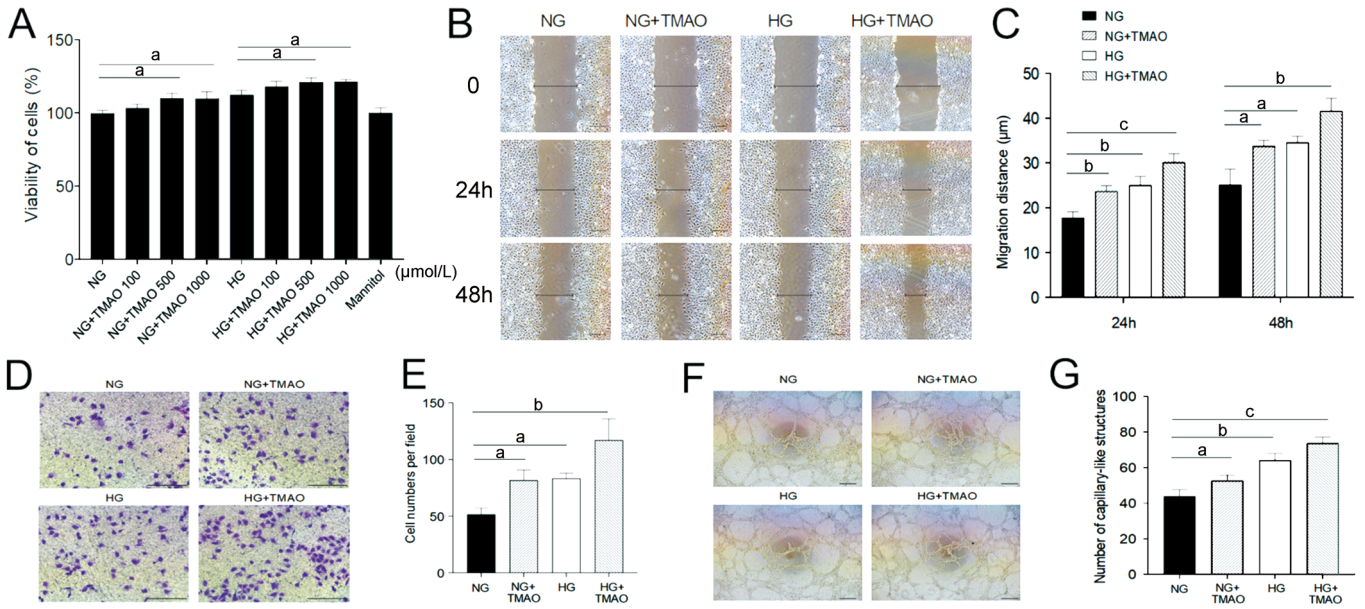

Figure 1 TMAO coordinates with high glucose to promote HRMEC proliferation, migration, and tube formation A: Cell proliferation of HREC under concentration series of glucose and TMAO. B, D, F: Wound healing, transwell and tube formation experiments of HREC under NG, HG, NG+TMAO and HG+TMAO conditions. Scale bar, 25 μm. C, E, G: Statistic analysis of wound healing, transwell and tube formation assays. NG: Normal glucose; NG+TMAO: Normal glucose+500 μmol/L TMAO; HG: High glucose; HG+TMAO: High glucose+500 μmol/L TMAO. TMAO: Trimethylamine N-oxide; HRMEC: Human retinal microvascular endothelial cells. ^{a}P<0.05, ^{b}P<0.01, ^{c}P<0.001. The representative results from three independent experiments are shown. Results are represented as means±SEM of data in triplicates.

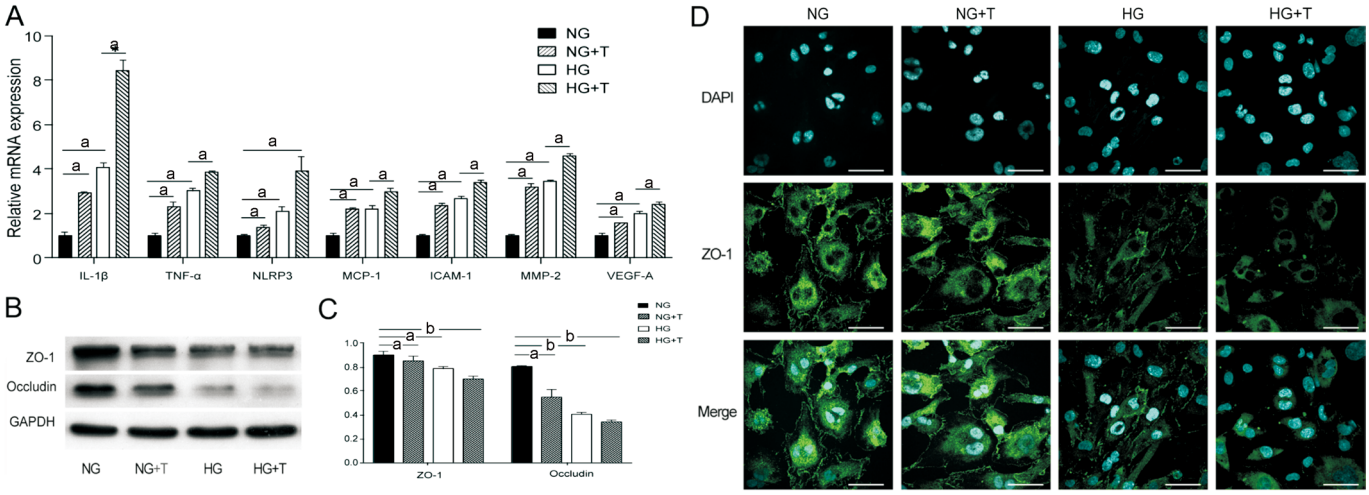

Figure 2 TMAO aggravates high glucose induced inflammation and cell junction loss in HRMEC A: Relative mRNA expression of ICAM-1, MCP-1, IL-1β, TNF-α, NLRP3, MMP-2, and VEGF-A of HRMEC under NG, NG+T, HG and HG+T conditions. B: Cell junction protein ZO-1 and occludin of HRMEC under concentration series of glucose and TMAO. C: Statistical analysis of ZO-1 and occludin protein expression in HRMEC under NG, NG+T, HG and HG+T conditions. D: ZO-1 (green) and DAPI (cyan) staining of HRMEC under NG, NG+T, HG and HG+T conditions. Scale bar, 50 μm. ^{a}P<0.05, ^{b}P<0.01. The representative results from three independent experiments are shown. Data are represented as means±SEM (n=3 for each group). NG: Normal glucose; NG+T: Normal glucose+500 μmol/L TMAO; HG: High glucose; HG+T: High glucose+500 μmol/L TMAO. TMAO: Trimethylamine N-oxide; HRMEC: Human retinal microvascular endothelial cells; IL-1β: Interleukin 1 beta; TNF-α: Tumor necrosis factor alpha; NLRP3: Nucleotide-binding oligomerization domain-like receptors 3; MCP-1: Monocyte chemoattractant protein 1; ICAM-1: Intercellular adhesion molecule 1; MMP-2: Matrix metallopeptidase 2; VEGF-A: Vascular endothelial growth factor A.

showed that compared to the NC group, the expression of VEGF was significantly increased in both the D group and the D+T group (P<0.01; Figure 5A, 5D). Moreover, the results of the WB analysis also suggested that the whole retina tight junction proteins ZO-1 and claudin-5 were dropped after TMAO intake (Figure 5A). ZO-1 expression was decreased in diabetic rats (P<0.05) and in T and D+T groups (P<0.01; Figure 5A-5B). Claudin-5 expression was inhibited in the T and D groups (P<0.05) and more significantly in the D+T group (P<0.01) compared to the NC group (Figure 5A, 5C).

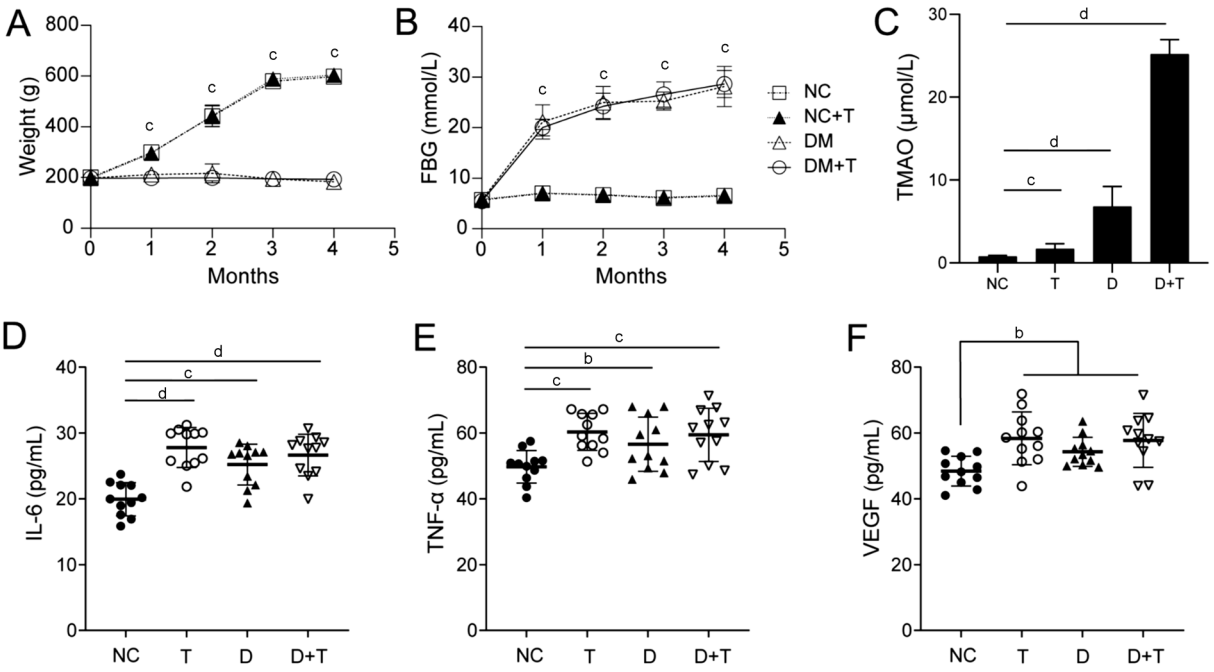

Figure 3 Circulating TMAO elevated in diabetic rats and induced systemic increase of IL-6, TNF-α and VEGF A, B: Evaluation of body weight and fast blood glucose of TMAO-treated, diabetic and diabetic rats treated with TMAO compared with normal rats. C: Plasma TMAO levels of the NC, T, D and D+T groups. D-F: The plasma IL-6, TNF-α, and VEGF concentrations of rats. [a]*P*<0.05, [b]*P*<0.01, [c]*P*<0.001, [d]*P*<0.0001. Results are represented as means±SEM (*n*>11 for each group). TMAO: Trimethylamine N-oxide; FBG: Fast blood glucose; NC: Negative control; T: TMAO; D: Diabetic mellitus; D+T: Diabetic mellitus+TMAO; IL-6: Interleukin 6; TNF-α: Tumor necrosis factor alpha; VEGF: Vascular endothelial growth factor.

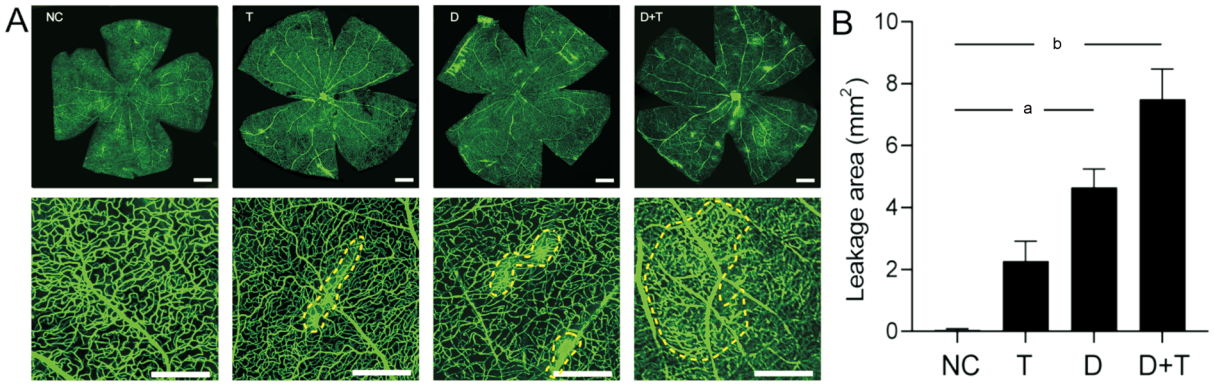

Figure 4 TMAO aggravates diabetic retinopathy by inducing vascular leakage A: The area of the rat retina blood vessel leakage was determined by fluorescein-labelled isothiocyanate dextran (FITC-dextran) infusion. The circled area shows the leakage area. Scale bar, 500 μm. B: Statistical analysis of the leakage areas of the rats' retinas. [a]*P*<0.05, [b]*P*<0.01. Results are represented as means±SEM (*n*=3 for each group). NC: Negative control; T: TMAO; D: Diabetic mellitus; D+T: Diabetic mellitus+TMAO; TMAO: Trimethylamine N-oxide.

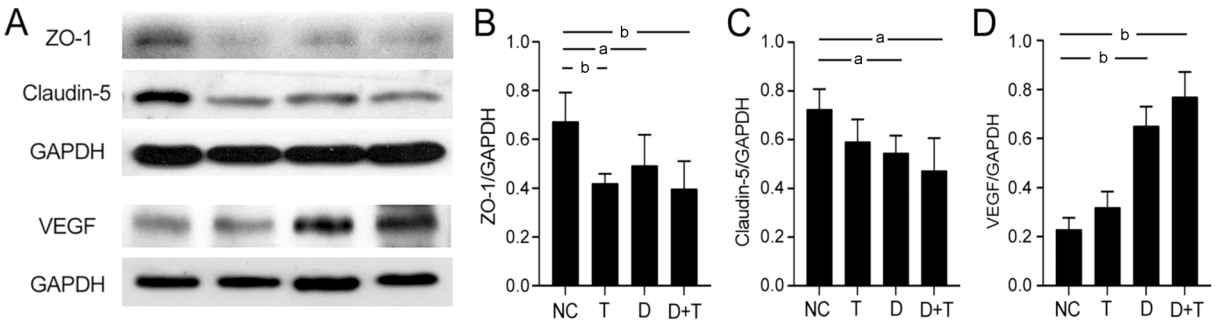

Figure 5 TMAO promotes destruction of cell junction proteins ZO-1 and claudin-5 and elevation of VEGF A: Western blotting of rat retina protein ZO-1, claudin-5, VEGF, and GAPDH. NC: Negative control; B, C, D: Statistical analysis of rat retina protein ZO-1, claudin-5, VEGF, and GAPDH. NC: Negative control; T: TMAO; D: Diabetic mellitus; D+T: Diabetic mellitus+TMAO. [a]*P*<0.05, [b]*P*<0.01. Results are represented as means±SEM (*n*=3 or 4 for each group). ZO-1: Zonula occludens-1; VEGF: Vascular endothelial growth factor; TMAO: Trimethylamine N-oxide.

DISCUSSION

The prevention of DR is a vital part of diabetes management and complication control. Although dietary intervention is considered an important approach to diabetic control, its role in DR still warrants increased attention. Plant-based diet patterns such as the Mediterranean diet may protect against the progression of DR[3]. The Western diet features red meat, and cholesterol negatively affects diabetes[17], but the association between the Western diet pattern and DR is still being delineated. Here, we propose that small molecules of TMAO that are rich in red meat may partly account for the development of DR. Prior studies found that TMAO is positively associated with increased risks of newly diagnosed type 2 diabetes[18], and act as a risk factor in diabetic patients[14,19]. Our previous work revealed that increased dietary choline intake was associated with higher risk of DR in females[20]. Moreover, our study revealed that there were higher plasma TMAO levels in DR patients, especially in patients with proliferative DR[11]. In the current study, we further investigated the specific role of TMAO in the development of DR through *in vitro* and *in vivo* experiments.

First, in our *in vitro* observation, we found TMAO increased vascular endothelium angiogenic ability from HRMEC proliferation, migration, and capillary-like structure formation, which may account for angiogenesis during DR. Although there are no published data concerning the effect of TMAO on HRMECs, studies on the impact of TMAO on vascular endothelial cells were contradictory. Some suggested TMAO as a proliferation enhancer[21], while others claimed that it impaired the self-repair capacity of human umbilical vein endothelial cells (HUVEC)[8]. The discrepancy may be due to the differential origin and gene expression between HRMEC and HUVEC[22]. HUVEC was derived from the human umbilical vein, while HRMEC was derived from human retinal microcapillary, which is more representative for DR. HUVEC indicated gene enrichment involving in embryological development, while ocular microvascular endothelial cells revealed an enrichment in major histocompatibility complex, immune response, and signal transduction.

Regardless of whether stimulated with pure TMAO or under HG culture conditions, TMAO exhibits the ability to promote the upregulation of inflammatory gene expression and adhesion factor expression in HRMECs. IL-1β and TNF-α can induce inflammation and apoptosis of endothelial cells, leading to endothelial cell injury and death, and causing abnormal proliferation and leakage of blood vessels[23]. ICAM-1 is an adhesion molecule that can increase the adhesion and infiltration of endothelial cells and inflammatory cells, leading to abnormal proliferation and leakage of retinal microvessels[24]. MCP-1 is a chemotactic factor that can attract inflammatory cells to the lesion area[25]. MMP-2, a member of matrix metalloproteinase family, degrades collagen and matrix molecules in the blood vessel wall, leading to increased fragility and leakage of the blood vessel wall[26]. IL-1β can also increase the expression of VEGF, promoting abnormal blood vessel neogenesis and proliferation. TNF-α can also increase the expression of MCP-1 and ICAM-1, further promoting the adhesion and infiltration of inflammatory cells. TMAO stimulation results in the overactivation and expression of the above genes, playing a role in the occurrence and development of DR.

Moreover, the literature report indicated that the biological function of TMAO is related to the concentration used. *In vitro* evidence showed that TMAO increased the pressure and temperature stability of folded proteins and biomolecular condensates by acting as chemical chaperons and reducing endoplasmic reticulum stress[27-28]. A pharmacological TMAO of 300 mmol/L acted as a suppressor of endoplasmic stress, while pathophysiological concentrations of TMAO at 50 μmol/L activated endoplasmic reticulum stress[29]. In our study, the mean plasma level of TMAO of diabetic and diabetic with TMAO supplement rats were 6.82 and 25.20 μmol/L, respectively, at which levels TMAO may result in deleterious effects on fundus.

Second, our results revealed TMAO associated with high glucose and caused a decline in tight junction protein ZO-1 and occludin in both HRMEC and retinas of diabetic rats. FITC-Dextran infusion confirmed a rise in retinal vascular leakage caused by TMAO and high blood glucose, which is consistent with clinical features during the onset of DR in diabetic patients.

Notably, a positive association between TMAO and the C-reactive protein was found by Meta-analysis[30]. In alignment with previous reports, ELISA results implied that TMAO intake promoted elevation of IL-6, TNF-α and VEGF in rat plasma. IL-6 and TNF-α both drive inflammation and cell junction breakdown in retinal vasculature[31]. Meanwhile, VEGF, acting as a common downstream factor of IL-6 and TNF-α, has been proven to activate nitric oxide synthase to disrupt tight junctional proteins such as zona occludens and occludin[32]. In DR, VEGF stimulate the proliferation and differentiation of endothelial cells in the retina, leading to abnormal angiogenesis and leakage[33]. Therefore, it is quite likely that TMAO impairs vascular integrity and accelerates progression of DR by inducing VEGF expression and systemic inflammation.

Third, we found that TMAO concentration in diabetic rats is higher than that of the normal group (*i.e.*, the group with standard chow and feeding water). Considerable evidence suggests that TMAO was mainly produced by gut microbiota

and excreted through urine[5]. Thus, we can reasonably speculate that the reduced glomerular filtration rate under diabetic conditions may increase the plasma TMAO level[34]. Also, the diabetic conditions may result in a shift of gut microbiota composition, which may lead to an increase of TMAO-producing flora and more TMAO emerging in plasma[35].

Our work has some limitations, and further evidence regarding the signal pathways by which TMAO perturbate iBRB and endothelial cells still requires further investigation. First, the level of IL-6 and TNF-α was measured in plasma rather than retina, while measurements of inflammatory factors at retinal transcription levels may give us more related hints, which could be included in further research. Second, the inhibition of downstream signal pathways may provide more solid evidence of the effect of TMAO on DR development and control. The circulating TMAO levels depend on factors including direct diet, precursor intake, gut microbiota metabolism, oxidase enzyme of liver and excretion ability[36]. TMAO was used as a biomarker of gut microbiota composition[37], but recent evidence suggests that TMAO alters gut microbiota homeostasis in turn[38]. Further studies may evaluate TMAO precursors and gut microbiome for biological insight into the human body.

In summary, TMAO coordinated with hyperglycaemia aggravates BRB impairment and vascular endothelial cell dysfunction in DR. There is growing potential for the use of inhibitors that target TMAO as a novel therapeutic strategy for the intervention of DR.

ACKNOWLEDGEMENTS

Foundations: Supported by the National Natural Science Foundation in China (No.81671641); Jiangsu Provincial Medical Innovation Team (No.CXTDA2017039); Gusu Health Talents Program (No.GSWS 2022018).

Conflicts of Interest: Jiang JY, None; **Liu WM,** None; **Zhang QP,** None; **Ren H,** None; **Yao QY,** None; **Liu GQ,** None; **Lu PR,** None.

REFERENCES

1 Stitt AW, Curtis TM, Chen M, Medina RJ, McKay GJ, Jenkins A, Gardiner TA, Lyons TJ, Hammes HP, Simó R, Lois N. The progress in understanding and treatment of diabetic retinopathy. *Prog Retin Eye Res* 2016;51:156-186.

2 Lu JY, Ma XJ, Zhou J, Zhang L, Mo YF, Ying LW, Lu W, Zhu W, Bao YQ, Vigersky RA, Jia WP. Association of time in range, as assessed by continuous glucose monitoring, with diabetic retinopathy in type 2 diabetes. *Diabetes Care* 2018;41(11):2370-2376.

3 Bryl A, Mrugacz M, Falkowski M, Zorena K. The effect of diet and lifestyle on the course of diabetic retinopathy-a review of the literature. *Nutrients* 2022;14(6):1252.

4 Jansson Sigfrids F, Dahlström EH, Forsblom C, Sandholm N, Harjutsalo V, Taskinen MR, Groop PH. Remnant cholesterol predicts progression of diabetic nephropathy and retinopathy in type 1 diabetes. *J Intern Med* 2021;290(3):632-645.

5 Bain MA, Fornasini G, Evans AM. Trimethylamine: metabolic, pharmacokinetic and safety aspects. *Curr Drug Metab* 2005;6(3):227-240.

6 Yoo W, Zieba JK, Foegeding NJ, Torres TP, Shelton CD, Shealy NG, Byndloss AJ, Cevallos SA, Gertz E, Tiffany CR, Thomas JD, Litvak Y, Nguyen H, Olsan EE, Bennett BJ, Rathmell JC, Major AS, Bäumler AJ, Byndloss MX. High-fat diet-induced colonocyte dysfunction escalates microbiota-derived trimethylamine *N*-oxide. *Science* 2021;373(6556):813-818.

7 Witkowski M, Weeks TL, Hazen SL. Gut microbiota and cardiovascular disease. *Circ Res* 2020;127(4):553-570.

8 Ma GH, Pan B, Chen Y, Guo CX, Zhao MM, Zheng LM, Chen BX. Trimethylamine N-oxide in atherogenesis: impairing endothelial self-repair capacity and enhancing monocyte adhesion. *Biosci Rep* 2017;37(2):BSR20160244.

9 Zhang XL, Li YN, Yang PZ, Liu XY, Lu LH, Chen YT, Zhong XL, Li ZH, Liu HL, Ou CW, Yan JY, Chen MS. Trimethylamine-N-oxide promotes vascular calcification through activation of NLRP3 (nucleotide-binding domain, leucine-rich-containing family, pyrin domain-containing-3) inflammasome and NF-κB (nuclear factor κB) signals. *Arterioscler Thromb Vasc Biol* 2020;40(3):751-765.

10 Dehghan P, Farhangi MA, Nikniaz L, Nikniaz Z, Asghari-Jafarabadi M. Gut microbiota-derived metabolite trimethylamine N-oxide (TMAO) potentially increases the risk of obesity in adults: an exploratory systematic review and dose-response meta- analysis. *Obes Rev* 2020;21(5):e12993.

11 Liu WM, Wang CM, Xia Y, Xia W, Liu GQ, Ren C, Gu Y, Li X, Lu PR. Elevated plasma trimethylamine-N-oxide levels are associated with diabetic retinopathy. *Acta Diabetol* 2021;58(2):221-229.

12 Aldana-Hernández P, Leonard KA, Zhao YY, Curtis JM, Field CJ, Jacobs RL. Dietary choline or trimethylamine N-oxide supplementation does not influence atherosclerosis development in ldlr$^{-/-}$ and apoe$^{-/-}$ male mice. *J Nutr* 2020;150(2):249-255.

13 He GD, Liu XC, Lu AS, Feng YQ. Association of choline intake with blood pressure and effects of its microbiota-dependent metabolite trimethylamine-N-oxide on hypertension. *Cardiovasc Ther* 2022;2022:9512401.

14 Fang Q, Zheng BJ, Liu N, Liu JF, Liu WH, Huang XY, Zeng XC, Chen LL, Li ZY, Ouyang DS. Trimethylamine N-oxide exacerbates renal inflammation and fibrosis in rats with diabetic kidney disease. *Front Physiol* 2021;12:682482.

15 Song B, Kim D, Nguyen NH, Roy S. Inhibition of diabetes-induced lysyl oxidase overexpression prevents retinal vascular lesions associated with diabetic retinopathy. *Invest Ophthalmol Vis Sci* 2018;59(15):5965-5972.

16 Oshitari T, Polewski P, Chadda M, Li AF, Sato T, Roy S. Effect of combined antisense oligonucleotides against high-glucose- and

diabetes-induced overexpression of extracellular matrix components and increased vascular permeability. *Diabetes* 2006;55(1):86-92.

17 Tanase DM, Gosav EM, Neculae E, Costea CF, Ciocoiu M, Hurjui LL, Tarniceriu CC, Maranduca MA, Lacatusu CM, Floria M, Serban IL. Role of gut microbiota on onset and progression of microvascular complications of type 2 diabetes (T2DM). *Nutrients* 2020;12(12):3719.

18 Shan ZL, Sun TP, Huang H, Chen SJ, Chen LK, Luo C, Yang W, Yang XF, Yao P, Cheng JQ, Hu FB, Liu LG. Association between microbiota-dependent metabolite trimethylamine- *N*-oxide and type 2 diabetes. *Am J Clin Nutr* 2017;106(3):888-894.

19 Iatcu CO, Steen A, Covasa M. Gut microbiota and complications of type-2 diabetes. *Nutrients* 2021;14(1):166.

20 Liu WM, Ren C, Zhang WP, Liu GQ, Lu PR. Association between dietary choline intake and diabetic retinopathy: national health and nutrition examination survey 2005-2008. *Curr Eye Res* 2022;47(2): 269-276.

21 Yang GL, Lin CC, Yang YW, Yuan L, Wang PL, Wen X, Pan MH, Zhao H, Ho CT, Li SM. Nobiletin prevents trimethylamine oxide-induced vascular inflammation via inhibition of the NF-κB/MAPK pathways. *J Agric Food Chem* 2019;67(22):6169-6176.

22 Browning AC, Halligan EP, Stewart EA, Swan DC, Dove R, Samaranayake GJ, Amoaku WM. Comparative gene expression profiling of human umbilical vein endothelial cells and ocular vascular endothelial cells. *Br J Ophthalmol* 2012;96(1):128-132.

23 Youngblood H, Robinson R, Sharma A, Sharma S. Proteomic biomarkers of retinal inflammation in diabetic retinopathy. *Int J Mol Sci* 2019;20(19):4755.

24 Siddiqui K, George TP, Mujammami M, Isnani A, Alfadda AA. The association of cell adhesion molecules and selectins (VCAM-1, ICAM-1, E-selectin, L-selectin, and P-selectin) with microvascular complications in patients with type 2 diabetes: a follow-up study. *Front Endocrinol* 2023;14:1072288.

25 Taghavi Y, Hassanshahi G, Kounis NG, Koniari I, Khorramdelazad H. Monocyte chemoattractant protein-1 (MCP-1/CCL2) in diabetic retinopathy: latest evidence and clinical considerations. *J Cell Commun Signal* 2019;13(4):451-462.

26 Saucedo L, Pfister IB, Zandi S, Gerhardt C, Garweg JG. Ocular TGF-*β*, matrix metalloproteinases, and TIMP-1 increase with the development and progression of diabetic retinopathy in type 2 diabetes mellitus. *Mediators Inflamm* 2021;2021:9811361.

27 Fischer H, Fukuda N, Barbry P, Illek B, Sartori C, Matthay MA. Partial restoration of defective chloride conductance in DeltaF508 CF mice by trimethylamine oxide. *Am J Physiol Lung Cell Mol Physiol* 2001;281(1):L52-L57.

28 Cinar S, Cinar H, Chan HS, Winter R. Pressure-sensitive and osmolyte-modulated liquid-liquid phase separation of eye-lens γ-crystallins. *J Am Chem Soc* 2019;141(18):7347-7354.

29 Chen SF, Henderson A, Petriello MC, *et al*. Trimethylamine N-oxide binds and activates PERK to promote metabolic dysfunction. *Cell Metab* 2019;30(6):1141-1151.e5.

30 MacPherson ME, Hov JR, Ueland T, Dahl TB, Kummen M, Otterdal K, Holm K, Berge RK, Mollnes TE, Trøseid M, Halvorsen B, Aukrust P, Fevang B, Jørgensen SF. Gut microbiota-dependent trimethylamine N-oxide associates with inflammation in common variable immunodeficiency. *Front Immunol* 2020;11:574500.

31 Lin CM, Titchenell PM, Keil JM, Garcia-Ocaña A, Bolinger MT, Abcouwer SF, Antonetti DA. Inhibition of atypical protein kinase C reduces inflammation-induced retinal vascular permeability. *Am J Pathol* 2018;188(10):2392-2405.

32 Bates DO. Vascular endothelial growth factors and vascular permeability. *Cardiovasc Res* 2010;87(2):262-271.

33 Capitão M, Soares R. Angiogenesis and inflammation crosstalk in diabetic retinopathy. *J Cell Biochem* 2016;117(11):2443-2453.

34 Mogensen CE, Hansen KW, Nielsen S, Pedersen MM, Rehling M, Schmitz A. Monitoring diabetic nephropathy: glomerular filtration rate and abnormal albuminuria in diabetic renal disease—reproducibility, progression, and efficacy of antihypertensive intervention. *Am J Kidney Dis* 1993;22(1):174-187.

35 Lemaitre RN, Jensen PN, Wang ZN, Fretts AM, McKnight B, Nemet I, Biggs ML, Sotoodehnia N, de Oliveira Otto MC, Psaty BM, Siscovick DS, Hazen SL, Mozaffarian D. Association of trimethylamine N-oxide and related metabolites in plasma and incident type 2 diabetes: the cardiovascular health study. *JAMA Netw Open* 2021;4(8):e2122844.

36 Ufnal M, Zadlo A, Ostaszewski R. TMAO: a small molecule of great expectations. *Nutrition* 2015;31(11-12):1317-1323.

37 Cho CE, Taesuwan S, Malysheva OV, Bender E, Tulchinsky NF, Yan J, Sutter JL, Caudill MA. Trimethylamine-N-oxide (TMAO) response to animal source foods varies among healthy young men and is influenced by their gut microbiota composition: a randomized controlled trial. *Mol Nutr Food Res* 2017;61(1):10.1002/mnfr.201600324.

38 Chen SY, Rong XY, Sun XY, Zou YR, Zhao C, Wang HJ. A novel trimethylamine oxide-induced model implicates gut microbiota-related mechanisms in frailty. *Front Cell Infect Microbiol* 2022;12:803082.